Article

Cell Reports

JNK Suppresses Tumor Formation via a Gene-Expression Program Mediated by ATF2

Graphical Abstract

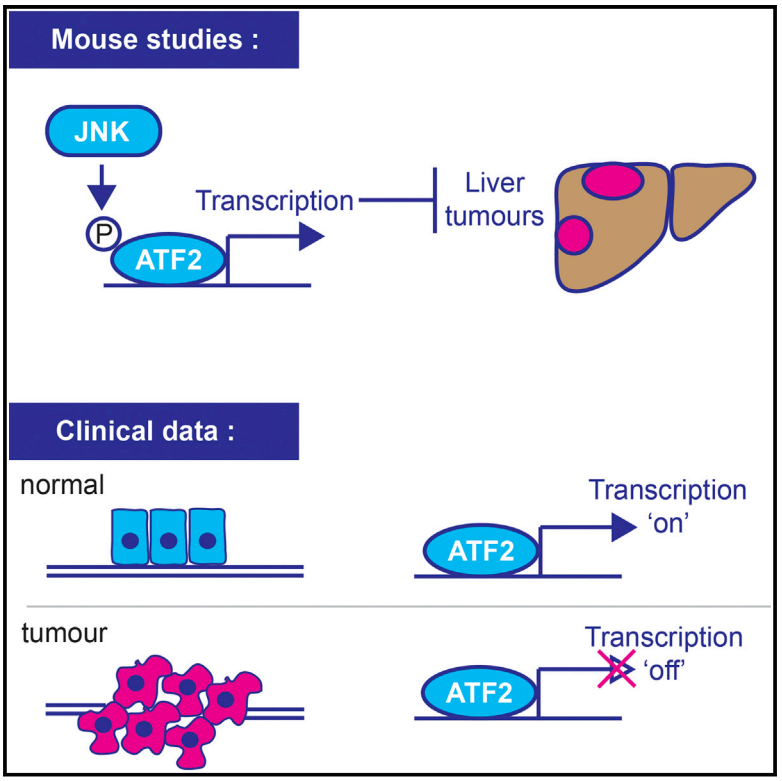

Authors

Malgorzata Gozdecka, Stephen Lyons, ..., Wolfgang Breitwieser, Nic Jones

Correspondence

nic.jones@cruk.manchester.ac.uk

In Brief

Given the large number of substrates phosphorylated by stress-activated kinases, identifying key effectors of their antitumorigenic function is a major challenge. Gozdecka et al. provide evidence that ATF2 mediates the tumor-suppressive effect of JNK through a transcriptional program that is frequently downregulated in human tumors.

Highlights

ATF2 suppresses tumor development in an orthotopic model of liver cancer

JNK activates ATF2, and suppression of liver tumorigenesis by JNK requires ATF2

We identify ATF2-regulated target genes capable of suppressing transformation

Underexpression of JNK-ATF2 targets is widespread in human tumors

Accession Numbers

GSE50530

Gozdecka et al., 2014, Cell Reports 9, 1361–1374
November 20, 2014 ©2014 The Authors
http://dx.doi.org/10.1016/j.celrep.2014.10.043

Cell Reports
Article

JNK Suppresses Tumor Formation via a Gene-Expression Program Mediated by ATF2

Malgorzata Gozdecka,[1,2,7] Stephen Lyons,[1,7] Saki Kondo,[1,3] Janet Taylor,[4,5] Yaoyong Li,[5] Jacek Walczynski,[1] Gerald Thiel,[6] Wolfgang Breitwieser,[1] and Nic Jones[1,*]
[1]Department of Cell Regulation, CRUK Manchester Institute, Paterson Building, University of Manchester, Manchester M20 4BX, UK
[2]Haematological Cancer Genetics, Wellcome Trust Sanger Institute, Wellcome Trust Genome Campus, Hinxton, Cambridge CB10 1SA, UK
[3]Laboratory of Molecular Genetics, Institute of Medical Science, University of Tokyo, 4-6-1 Shirokanedai, Minato-ku, Tokyo 108-8639, Japan
[4]Central Manchester NHS Trust and University of Manchester, the Nowgen Centre, 29 Grafton Street, Manchester M13 9WU, UK
[5]Applied Computational Biology and Bioinformatics Group, CRUK Manchester Institute, Paterson Building, University of Manchester, Manchester M20 4BX, UK
[6]Department of Medical Biochemistry and Molecular Biology, University of Saarland Medical Center, Building 44, 66421 Homburg, Germany
[7]Co-first author
*Correspondence: nic.jones@cruk.manchester.ac.uk
http://dx.doi.org/10.1016/j.celrep.2014.10.043

SUMMARY

JNK and p38 phosphorylate a diverse set of substrates and, consequently, can act in a context-dependent manner to either promote or inhibit tumor growth. Elucidating the functions of specific substrates of JNK and p38 is therefore critical for our understanding of these kinases in cancer. ATF2 is a phosphorylation-dependent transcription factor and substrate of both JNK and p38. Here, we show ATF2 suppresses tumor formation in an orthotopic model of liver cancer and cellular transformation in vitro. Furthermore, we find that suppression of tumorigenesis by JNK requires ATF2. We identify a transcriptional program activated by JNK via ATF2 and provide examples of JNK- and ATF2-dependent genes that block cellular transformation. Significantly, we also show that ATF2-dependent gene expression is frequently downregulated in human cancers, indicating that amelioration of JNK-ATF2-mediated suppression may be a common event during tumor development.

INTRODUCTION

The stress-activated kinases JNK and p38 play an essential role in the cellular response to a number of different extracellular and intracellular signals including exposure to cytokines, growth factors, and various stresses. They regulate many key biological processes, such as cellular proliferation and death, which function aberrantly in cancer. Accordingly, these kinases are proposed to have critical roles in tumor development (Wagner and Nebreda, 2009). However, the complexity of stress-dependent signaling networks means that JNK and p38 have both pro- and antitumorigenic functions. Consistent with a protumorigenic role, these kinases are frequently found to be highly activated in human cancers and to support the proliferation of tumor-derived cell lines (Esteva et al., 2004; Hui et al., 2008; Salh et al., 2002; Yang et al., 2003). Conversely, comprehensive analysis of cancer genomes has revealed inactivating mutations in several kinases lying upstream of JNK and p38, strongly implying a tumor-suppressive role for these pathways. For example, a recent survey of breast cancer genomes revealed mutations in MEKK1 in 6% of cancers, most of which resulted in protein truncation. In this same study, LZK1 was also found to be mutated in some breast cancers (Stephens et al., 2012). ASK1 and MLK1 have been reported to be frequently mutated in melanomas (Stark et al., 2012), leading to loss of their function, and the MAP2 kinase MKK4, which directly activates JNK and p38, has been identified as a "cancer gene" on the basis of its frequent mutation in several cancers (Greenman et al., 2007).

The role of JNK and p38 in tumorigenesis has been studied in a variety of mouse tumor models. p38 is inhibitory to oncogenic Ras-mediated transformation in vitro (Dolado et al., 2007) as well as liver and lung tumorigenesis in vivo (Hui et al., 2007; Ventura et al., 2007). These studies support a tumor-suppressive role for p38. The role of JNK is more complex, and depending on the experimental setting, this kinase either promotes or antagonizes tumorigenesis in mice. For example, studies using $JNK1^{-/-}$ mice indicate that JNK1 facilitates DEN-induced liver tumor formation (Eferl et al., 2003; Hui et al., 2008; Sakurai et al., 2006). However, JNK drives liver tumorigenesis by promoting expression of hepatic cytokines in nonparenchymal liver cells, and deletion of JNK specifically in hepatocytes reveals its suppressive role in liver tumor development (Das et al., 2011). Furthermore, although JNK supports tumor growth in some tissues such as lung and gastric cancer (Cellurale et al., 2011; Shibata et al., 2008), it exhibits potent tumor-suppressive properties in mouse models of prostate and breast cancer (Cellurale et al., 2010, 2012; Hübner et al., 2012). Thus, a complex picture emerges, in which JNK and p38 function in a context-dependent manner to regulate tumorigenesis. In order to unravel such complexity, a better understanding of the role of effector substrates for the stress-activated protein kinases is required.

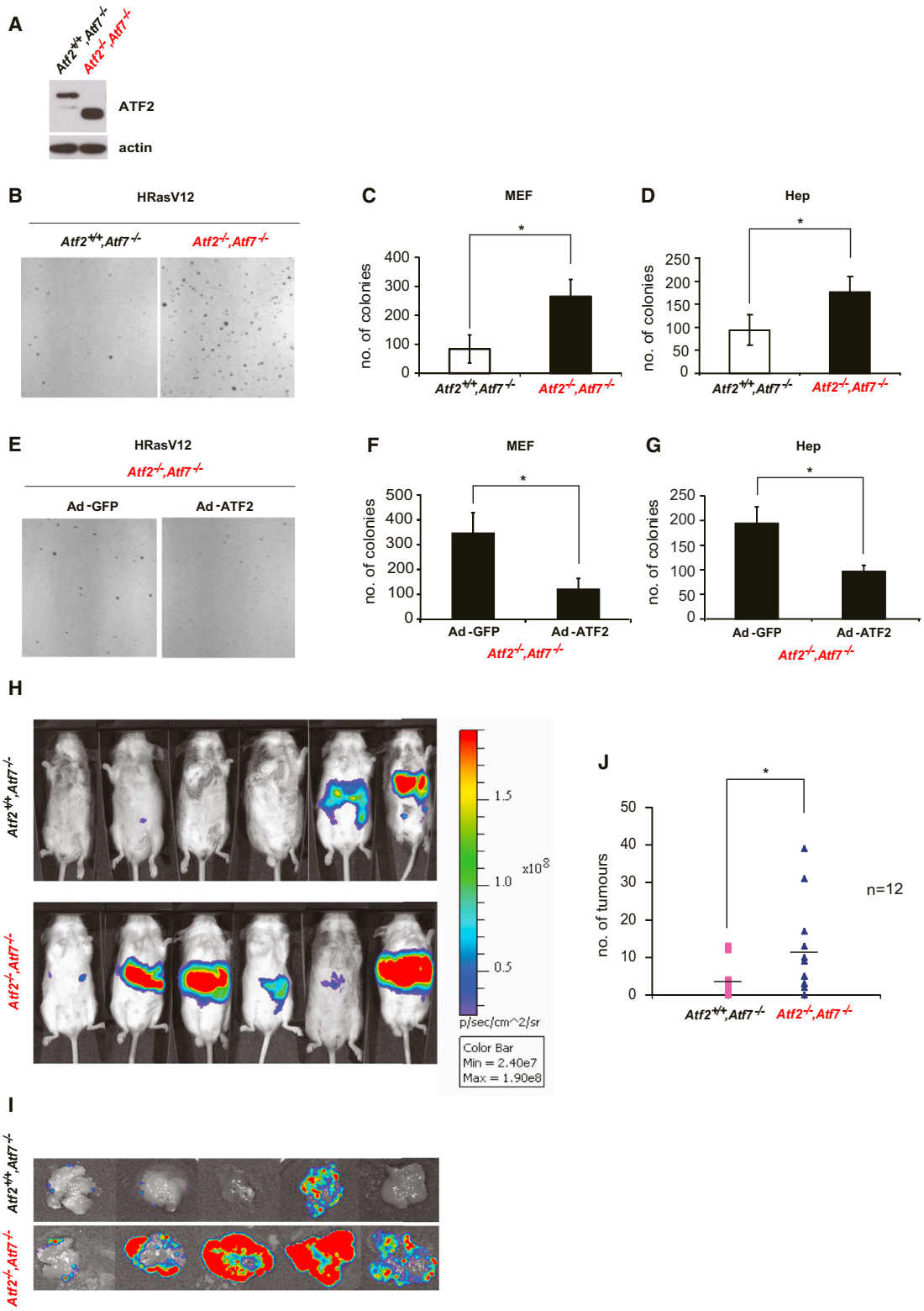

Figure 1. Suppression of Ras-Mediated Transformation and Liver Tumorigenesis by ATF2

(A) Extracts from *Atf2* WT (Atf2$^{+/+}$, Atf7$^{-/-}$, and p53$^{-/-}$) and Atf2 KO (Atf2$^{-/-}$, Atf7$^{-/-}$, and p53$^{-/-}$) hepatoblasts were immunoblotted for ATF2 and β-actin. (B–D) Anchorage-independent growth of HRasV12-expressing *Atf2* WT and KO MEFs (B and C) and hepatoblasts (D). Values plotted are numbers of colonies per dish; ± SD; n = 18 (three experiments × six dishes per experiment); *p < 0.05.

(legend continued on next page)

JNK and p38 have many downstream targets including a diverse set of transcription factors through which they can initiate complex changes to gene expression. ATF2 is a substrate of both JNK and p38 and belongs to the AP-1 family of B-Zip-containing transcription factors. In response to diverse stimuli, these kinases phosphorylate ATF2 at two key threonine residues in the N-terminal transactivation domain (TAD), leading to its activation (Gupta et al., 1995). Several studies have implicated ATF2 in cancer. High levels of phospho-ATF2 have been detected in human melanoma samples, and a role for ATF2 in driving progression of these tumors has been suggested (Berger et al., 2003; Shah et al., 2010). Conversely, ATF2 can inhibit tumor formation in some settings. After a latency period of 60 weeks, ATF2 heterozygous mice develop mammary tumors spontaneously, and furthermore, low levels of ATF2 expression in human breast tumors have been reported (Maekawa et al., 2007). ATF2 also inhibits tumor development in a mouse model of skin cancer (Bhoumik et al., 2008), and deletion of ATF2 in B cells leads to a resistance to apoptosis and accelerates the onset of lymphoma in the Eμ-Myc mouse model (Walczynski et al., 2014). Furthermore, recent findings indicate that the SS18-SSX2 fusion protein found in human synovial sarcomas derives its oncogenicity from its ability to interact with ATF2 and to silence ATF2 target promoters (Su et al., 2012).

In this study, we sought to clarify the role of ATF2, and its requirement for JNK and p38 signaling, in cellular transformation and tumorigenesis. By using an orthotopic model of liver cancer, we demonstrate a tumor-suppression role for JNK, which is effected via activation of ATF2-dependent transcription. Furthermore, we define an ATF2-dependent gene signature that is decreased in several types of human cancer, consistent with a tumor-suppressive role for JNK-ATF2 signaling.

RESULTS

ATF2 Suppresses Ras-Dependent Cellular Transformation and Liver Tumorigenesis

To investigate the effect of ATF2 on oncogenic HRas-mediated transformation, we utilized mouse embryonic fibroblasts (MEFs), which allow for the conditional deletion of the ATF2 DNA-binding domain ($Atf2^{Flox/Flox}$). ATF2 shares overlapping functions with ATF7 during development (Breitwieser et al., 2007). To eliminate the potential for redundancy, we deleted ATF7 by crossing $Atf2^{Flox/Flox}$ mice with $Atf7^{-/-}$ mice. To render the cells susceptible to HRasV12-mediated transformation, we deleted p53 by crossing $Atf2^{Flox/Flox}$, $Atf7^{-/-}$ mice with $p53^{-/-}$ mice. Deletion of *Atf2* was achieved in vitro by transient expression of Cre recombinase, using an adenoviral vector. This approach led to complete deletion of the ATF2 DNA-binding domain, generating cells with the genotype $Atf2^{-/-}$, $Atf7^{-/-}$, $p53^{-/-}$, referred to hereafter as *Atf2* knockout (KO). Cells treated with a control vector continue to express full-length ATF2 protein and are referred to hereafter as *Atf2* wild-type (WT) ($Atf2^{+/+}$, $Atf7^{-/-}$, $p53^{-/-}$; Figure 1A).

To assess the role of ATF2 in cellular transformation, we compared the growth of HRasV12-expressing *Atf2* WT and *Atf2* KO MEFs in soft agar. *Atf2* KO cells gave rise to significantly greater numbers of colonies than did wild-type controls, indicating that ATF2 suppresses cellular transformation (Figures 1B and 1C). Re-expression of ATF2 in Ras-transformed *Atf2* KO MEFs impaired colony formation, confirming that the observed phenotype was due to loss of ATF2 (Figures 1E and 1F). Notably, in the absence of HRasV12, *Atf2* KO cells did not form colonies in soft agar (Figure S1A), showing that loss of ATF2 is not sufficient for transformation.

We next studied the role of ATF2 in tumor development in vivo using an orthotopic mouse model of hepatocellular carcinoma, which involves transformation of embryonic hepatoblasts in vitro and their subsequent injection into preconditioned recipient mice (Zender et al., 2006). Similarly to MEFs, *Atf2* KO hepatoblasts displayed enhanced colony formation in soft agar (Figure 1D), which was efficiently rescued by re-expression of ATF2 (Figure 1G). Although anchorage-independent growth of *Atf2* KO cells was enhanced, adherent growth was not significantly affected (Figures S1B and S1C).

Next, HRasV12-transformed *Atf2* KO and *Atf2* WT hepatoblasts were introduced into the spleen of recipient mice, from where they home to the liver. Tumor growth was assessed 14 days later using luciferase-dependent luminescence. Prior to injection, bioluminescence of *Atf2* WT and KO cells was similar (Figure S1D). However, a significantly higher level of bioluminescence was observed in the mice injected with HRasV12-transformed *Atf2* KO cells, indicating greater tumor growth (Figure 1H). Analysis of dissected livers confirmed the presence of large tumor masses in all (6/6) mice injected with *Atf2* KO cells. In comparison, in the *Atf2* WT group, tumor growth was reduced and detected in only four of the six recipient mice (Figure 1I). Both *Atf2* WT and KO cells formed trabecular, pseudoglandular, and solid histological tumor types typical of human hepatocellular carcinoma (HCC) (not shown).

To enumerate tumors, the experiment was repeated with fewer hepatoblasts being injected, and livers were assessed after 6 weeks. Multiple small tumor nodules were observed in 92% (11/12) of recipient mice injected with *Atf2* KO cells and 75% (9/12) of recipient mice injected with *Atf2* WT cells. However, *Atf2* KO cells generated approximately 3-fold more tumor nodules (Figure 1J). Thus, both the number and size of tumors was greater in the absence of ATF2, indicating that ATF2 suppresses HRasV12-driven liver tumorigenesis.

(E–G) HRasV12-expressing *Atf2* KO MEFs (F) or hepatoblasts (E and G) were transduced with recombinant adenoviruses (Ad-) expressing either ATF2 or GFP as indicated; n = 18; ± SD; *p < 0.05.

(H) Bioluminescence imaging of mice injected with HRasV12- and luciferase-expressing *Atf2* WT (upper panel) and *Atf2* KO (lower panel) hepatoblasts (1.5×10^6 cells/mouse; n = 6). Mice were imaged 14 days after cell injection.

(I) Bioluminescence of resected livers at day 14.

(J) Quantification of liver tumors. HRasV12- and luciferase-expressing *Atf2* WT and *Atf2* KO hepatoblasts were injected into the spleen of recipient mice (0.2×10^6 cells/mouse; n = 12). *p < 0.05. Tumor nodules were enumerated 6 weeks after cell transplantation.

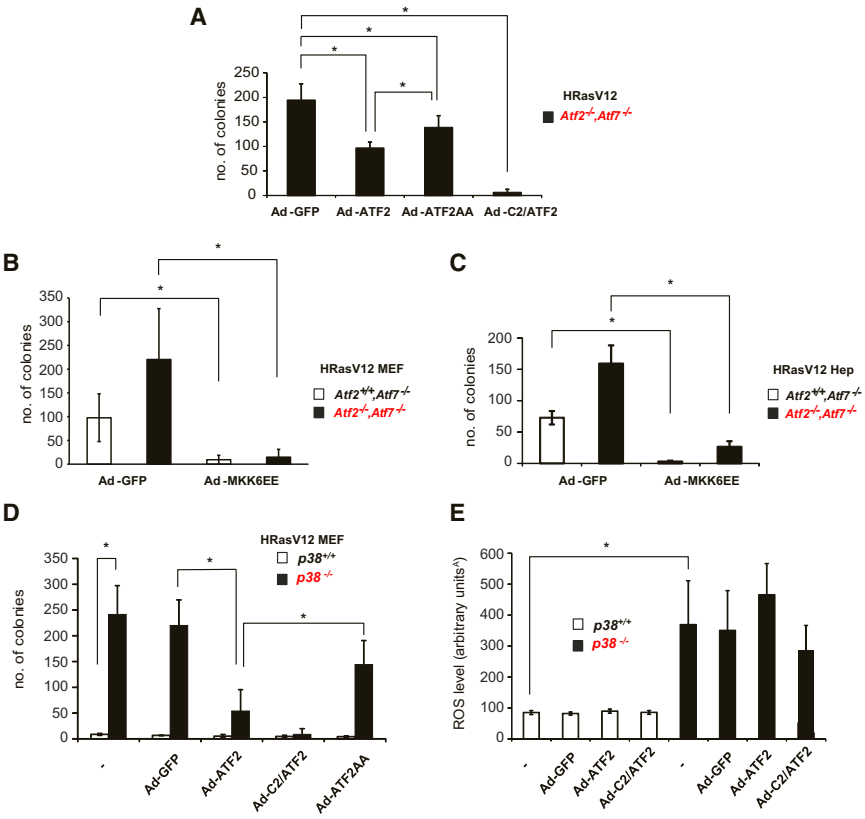

Figure 2. p38 MAPK Is Not Required for ATF2-Mediated Suppression of Ras Transformation

(A) HRasV12-expressing *Atf2* KO hepatoblasts were transduced with Ad-ATF2, Ad-ATF2-AA, Ad-C2/ATF2, or Ad-GFP, and colony formation in soft agar was assessed. ± SD; n = 18; *p < 0.05.

(B and C) HRasV12-expressing *Atf2* WT and KO MEFs (B) or hepatoblasts (C) were transduced with Ad-MKK6EE or Ad-GFP, and anchorage-independent growth was analyzed. ± SD; n = 18; *p < 0.05.

(D) Anchorage-independent growth of HRasV12-expressing p38 WT and KO MEFs transduced with Ad-ATF2, Ad-C2/ATF2, Ad-ATF2AA, and Ad-GFP. ± SD; n = 18; *p < 0.05.

(E) p38α WT and KO cells transduced with either Babe-HRasV12 or Babe-Empty control retrovirus were treated with Ad-GFP, Ad-ATF2, and Ad-C2A. FACS analysis, employing a redox-sensitive fluorophore, dihydroethidium (DHE), was used to detect cellular ROS. ROS levels were calculated as (BABE-RAS mean DHE fluorescence/BABE mean DHE fluorescence) × 100. ± SD; n = 3; *p < 0.05.

Phosphorylation of the ATF2 TAD Is Required for Suppression of HRasV12-Dependent Transformation

To examine the role of the ATF2 TAD in suppression of oncogenic Ras-mediated transformation, we generated an adenoviral vector expressing a mutant ATF2, wherein two key mitogen-activated protein (MAP) kinase phosphorylation sites are changed to alanine (ATF2AA). This mutant is transcriptionally inactive (Figures S2A and S2B). Unlike wild-type ATF2, ATF2AA was unable to efficiently suppress colony formation in soft agar, indicating that phosphorylation of the TAD is important for suppression of HRasV12-dependent transformation by ATF2 (Figure 2A). In addition, we constructed an adenoviral vector expressing a constitutively active form of ATF2 (C2/ATF2; Steinmüller and Thiel, 2003), which does not require stress-dependent phosphorylation for its activity (Figures S2C and S2D). When expressed in Ras-transformed *Atf2* KO cells, C2/ATF2 markedly suppressed anchorage-independent growth (Figure 2A). These lines of evidence demonstrate that ATF2-dependent suppression of cellular transformation is dependent upon transcriptional activation.

ATF2-Mediated Suppression of Ras-Mediated Transformation Is Independent of p38 MAP Kinase

Both JNK and p38 efficiently phosphorylate ATF2 and can suppress cellular transformation and tumor development. To address the potential role of p38, we utilized an activated mutant of *Map2k6* (MKK6EE), which activates p38 specifically. MKK6EE efficiently suppressed colony formation in both *Atf2* WT and *Atf2* KO MEFs (Figure 2B) and hepatoblasts (Figure 2C), showing that, in this setting, p38 does not require ATF2 to mediate its suppressive activity. *p38α* knockout MEFs form greater numbers of colonies in soft agar than *p38* WT MEFs when transformed by oncogenic Ras (Dolado et al., 2007). ATF2 strongly impaired this enhanced colony formation of *p38α* KO cells (Figure 2D), showing that ATF2 does not require p38α-mediated phosphorylation for the suppression of transformation. Notably, suppression by ATF2-AA was impaired (Figures 2D and S2E), confirming that phosphorylation of ATF2 is required for suppression of transformation and, further, that this phosphorylation must still occur in *p38α* knockout cells. Given that p38α has been shown to suppress Ras transformation by lowering intracellular reactive oxygen species (ROS) levels (Dolado et al., 2007), we asked whether ATF2 also suppresses colony formation by controlling ROS. As expected, *p38α* knockout cells generated high levels of ROS in response to HRasV12 transformation (Figure 2E), but ATF2 expression had no influence on these elevated ROS levels (Figure 2E). Thus, ATF2 and p38 can suppress transformation independently of each other and by distinct mechanisms.

JNK Is Required for ATF2 Function

In response to a range of stresses, ATF2 was efficiently phosphorylated in *p38α* knockout cells (Figure S3A) but was sensitive to specific JNK inhibition (Figure S3B). To further confirm this finding, ATF2 phosphorylation was examined in *Jnk1/2* WT (*Jnk1/2*$^{+/+}$, *p53*$^{-/-}$) and *Jnk1/2* KO (*Jnk1/2*$^{-/-}$, *p53*$^{-/-}$) MEFs. Loss of JNK led to a severe impairment of ATF2 phosphorylation despite the fact that p38 was strongly activated in response to stress (Figure S3C). Furthermore, binding of ATF2 to the c-Jun promoter, a known target gene, was impaired in *Jnk1/2* KO cells

(Figure S3D). Thus, JNK is indispensable for ATF2 function, strongly indicating that suppression of tumorigenesis by ATF2 is likely to be JNK dependent.

JNK1 Suppresses Oncogenic Ras-Mediated Transformation via ATF2

Because ATF2 inhibited formation of liver tumors and requires JNK for activation, we asked whether ATF2 is required for tumor suppression by the JNK pathway. Expression of constitutively active JNK (JNK1-CA; Lei et al., 2002) significantly elevated the level of ATF2 phosphorylation in Ras-transformed NIH 3T3 cells (Figure S3E) compared to GFP and kinase-dead JNK controls. Phosphorylation of c-Jun by JNK-CA was also observed (Figure S3E). Expression of JNK1-CA in HRasV12-transformed NIH 3T3 cells significantly suppressed colony formation whereas JNK1-KD or GFP had no effect (Figure 3A). Thus, although genetic ablation of JNK renders cells resistant to Ras transformation (Cellurale et al., 2011), increased JNK activity causes phosphorylation of its downstream substrates and impairs Ras-dependent transformation.

Next, we asked whether JNK1-CA suppresses transformation and tumorigenesis via ATF2. JNK1-CA strongly suppressed colony formation in *Atf2* WT cells whereas only minor suppression was observed in the *Atf2* KO cells (Figures 3B and 3C). Expression of JNK1-KD had no effect on colony formation in soft agar (Figures 3B and 3C). Equal expression of JNK-CA in *Atf2* WT and *Atf2* KO cells was confirmed by western blot analysis (Figure S3F). Furthermore, re-expression of ATF2 in *Atf2* KO cells restored JNK1-CA-mediated suppression of transformation (Figure 3D). Consistent with these findings, we observed a marked suppression of liver tumorigenesis by JNK1-CA when expressed in *Atf2* WT, but not *Atf2* KO cells (Figure S3G). Furthermore, re-expression of ATF2 in *Atf2* KO cells together with JNK1-CA resulted in strong suppression of liver tumorigenesis, whereas coexpression of JNK1-CA and GFP resulted only in a modest reduction (Figures 3E and S3H). These results indicate that JNK activity suppresses liver tumorigenesis in vivo and requires ATF2.

The Cellular Response to ATF2 Activation and Identification of ATF2-Dependent Transcriptional Targets

To identify ATF2 transcriptional targets involved in cellular transformation, we carried out gene-expression profiling, employing constitutively active ATF2 (C2/ATF2), which allows for the expression of ATF2 targets in the absence of stress (Figures S2C and S2D).

First, we assessed the biological consequences of ATF2-dependent gene expression. Expression of C2/ATF2 in hepatoblasts led to a striking loss of cellular proliferation within 16 hr (Figures 4A and 4B), and within 48 hr, we observed the onset of cell death detected by annexin V staining (Figures 4C and 4D). Note that expression of WT ATF2 did not affect cell viability (Figure 4D), consistent with our observation that overexpression of ATF2 does not induce target gene expression unless accompanied by stress (Figures S2A and S2B). Treatment of C2/ATF2-transduced cells with cycloheximide (Figures 4E and 4F) or actinomycin D (data not shown) significantly blocked the induction of apoptosis, suggesting that target gene expression is required for the induction of cell death by active ATF2.

To identify ATF2 target genes, we expressed C2/ATF2 or GFP in hepatoblasts for 8 hr and performed microarray analysis. Employing a threshold of a 3-fold or greater change in expression, we observed 270 differentially expressed genes (244 up- and 26 downregulated; $p < 0.01$) including previously reported ATF2 targets, e.g., *ATF3*, *DUSP10*, and *JUN*. Next, we confirmed that the microarray strategy successfully identified authentic targets of wild-type ATF2. We selected a subset of genes, all of which were induced by 4-fold or greater in the microarray experiment, and confirmed that the majority of these selected genes were dependent on ATF2 for their expression by comparing their transcript levels in *Atf2* WT versus *Atf2* KO cells, in the presence or absence of methyl methanesulfonate (MMS) stress, using quantitative RT-PCR (qRT-PCR) (Table S1). Because JNK activity is critical for ATF2 activation (Figure S3C), we compared the expression of ATF2-dependent genes in *Jnk1/2* WT versus *Jnk1/2* KO MEFs and found that the majority of these were expressed in a JNK-dependent manner (Table S2). Furthermore, analysis of chromatin immunoprecipitation sequencing (ChIP-seq) data in the ENCODE database (Thomas et al., 2007) confirmed the presence of ATF2-binding sites in 219 out of 270 genes from the microarray gene set (Table S3), suggesting that the majority of genes we identified are direct targets of ATF2.

As presented in Figure 3, expression of active JNK led to inhibition of tumorigenesis in an ATF2-dependent manner. To assess ATF2 target gene expression under these conditions, we expressed JNK1-CA together with ATF2, ATF2-AA, or GFP in *Atf2* KO cells and measured the expression of genes selected from the microarray data by qRT-PCR. JNK1-CA displayed limited or no ability to induce expression of the microarray targets when expressed in *Atf2* KO cells. On the other hand, coexpression of JNK1-CA with ATF2 led to a significant induction of several of the identified targets (Table S4). This induction depended entirely on the phosphorylation of ATF2, because coexpression of JNK1-CA and ATF2-AA did not lead to transactivation of the targets. Thus, we identified a set of genes whose expression is induced by JNK via phosphorylation of ATF2.

Inhibition of Cellular Transformation by Selected JNK-ATF2-Dependent Target Genes

Next, we wished to ascertain whether any of the identified genes were capable of suppressing cellular transformation mediated by oncogenic Ras. We selected six candidate genes for further analysis. Each of the genes was confirmed to be a transcriptional target of JNK signaling via ATF2. Thus, their expression is impaired in *Atf2* KO cells versus WT controls (Figure 5A) and in JNK1/2 KO MEFs versus WT controls (Figure 5B; note, however, that *NTS* expression was not reduced in JNK1/2 KO cells). In addition, expression of each of these genes was induced by JNK1-CA via phosphorylation of ATF2 (Figure 5C). HRasV12-transformed *Atf2* WT and KO MEFs were infected either with adenoviruses expressing each of the JNK-ATF2-dependent targets or a GFP-expressing control. Subsequently, the efficiency of cellular transformation was monitored by assessing colony formation in soft agar. Expression of three of the candidates

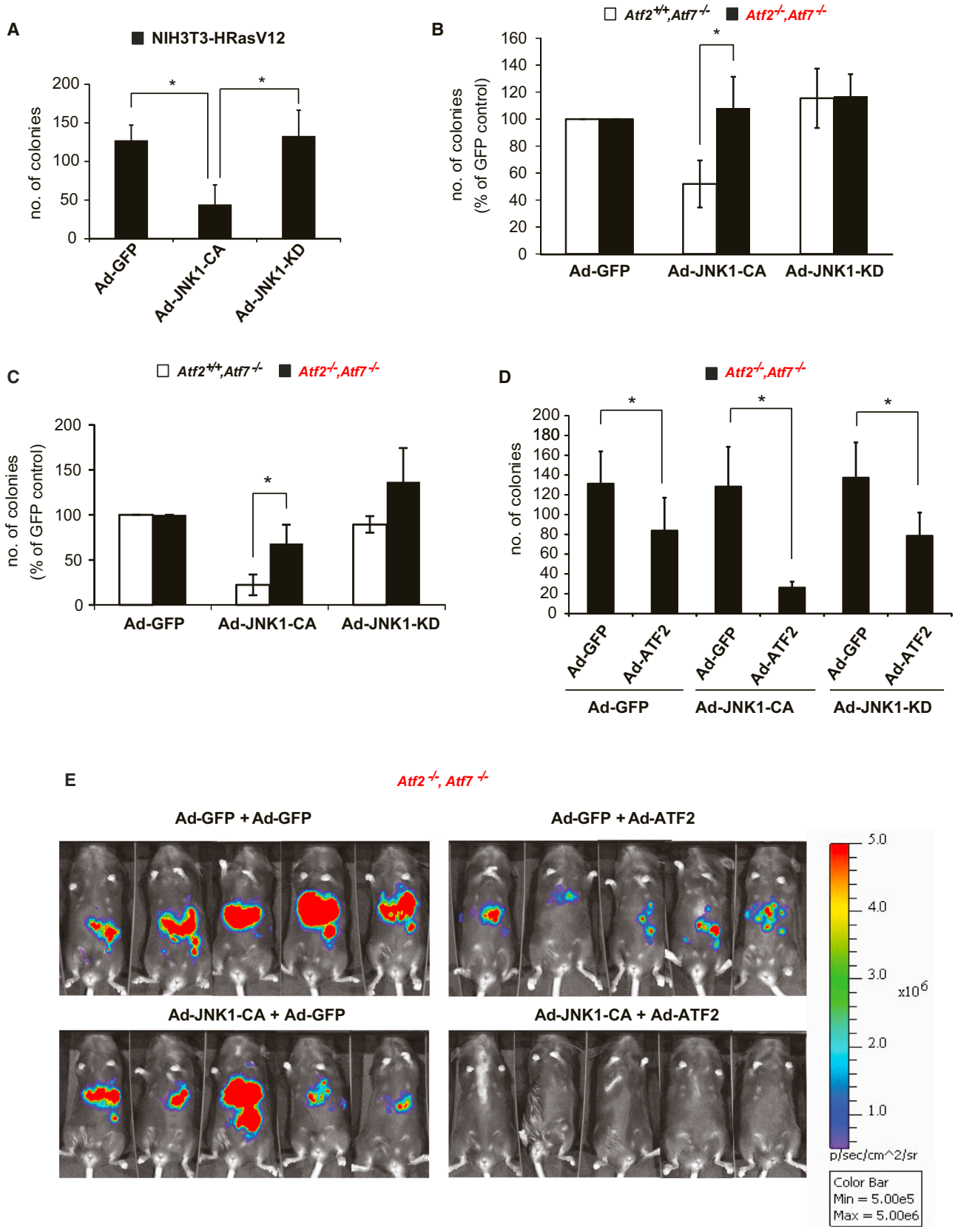

(legend on next page)

(*PPP2R5B*, *GABRA1*, and *RCAN1*) suppressed colony formation (Figure 6A). Although some suppression of colony formation was observed in *Atf2* WT MEFs, the suppression was most clearly observed in *Atf2* KO MEFs, where exogenous expression of each of these genes substantially suppressed the *Atf2* KO phenotype. As shown in Figure 6B, expression of *GABRA1* induced apoptosis in both *Atf2* WT and KO cultures, which may account for its ability to impair anchorage-independent growth. On the other hand, expression of neither *PPP2R5B* nor *RCAN1* induced significant amounts of apoptosis, indicating that these genes likely inhibit transformation by another mechanism. Therefore, we measured the effect of expressing *PPP2R5B* and *RCAN1* on cell-cycle progression and found that both genes led to a reduction of cells in S phase (Figures 6C and 6D). Interestingly, whereas *PPP2R5B* expression increased the number of cells in G1/G0, Rcan1 caused cells to accumulate in G2. These data identify transcriptional targets of ATF2 that are either proapoptotic or antiproliferative and capable of inhibiting HRasV12-mediated cellular transformation.

JNK- and ATF2-Dependent Transcripts Are Underexpressed in Human Tumors

To determine whether our findings are relevant to human tumor development, we examined the expression of ATF2-dependent transcriptional targets in human tumors through interrogation of tumor-derived transcriptomic data available in the public domain.

First, we examined expression of ATF2 targets in human HCC. We observed that RCAN1 expression was markedly downregulated in HCCs when compared to normal tissue in three independent studies, consistent with a tumor-suppressive role of ATF2 in HCC (Figure 7A). In addition, we noted that *PPP2R5B* and *GABRA1* were also underexpressed in HCC samples (Figure S4).

To obtain a more-comprehensive picture of the behavior of ATF2-dependent transcripts in tumors, we used our microarray data to compile an ATF2 gene signature comprising 31 genes. Each gene in the signature was shown to be induced by JNK-mediated phosphorylation of ATF2 as shown in Table S4. Next, we analyzed the Oncomine data set, comparing expression of the ATF2 gene signature in normal tissue versus tumor samples, expanding the analysis to encompass all tumor types. We observed a significant ($p < 0.001$) overlap between the ATF2 gene signature and the top-ranking (1%–10%) underexpressed genes in 8/20 cancer types, including brain, breast, colorectal, and lung (Table S5). Notably, in no case was the ATF2 gene set significantly overexpressed. The downregulation of ATF2 targets was particularly striking in breast cancers. As an example, the heatmap presented in Figure 7B illustrates the reduced expression of the ATF2 gene signature in mucinous breast carcinomas analyzed by Curtis et al. (2012). For this data set, 13 of the 31 genes comprising the ATF2 gene signature fell within the top 10% of underexpressed genes in tumor versus normal samples. In addition, we identified several ATF2 targets (including *RCAN1*) that are consistently downregulated in ductal and lobular tumors, as well as the rarer medullary, tubular, and mucinous breast cancer types (Figure 7C). Furthermore, ATF2 targets were underexpressed in ductal carcinoma in situ samples, indicating that loss of their expression may be an early event in development of breast tumors. The underexpression of ATF2 targets was also evident in breast cancer data from The Cancer Genome Atlas study (Figure 7D). Thus, loss of ATF2-dependent transcription appears to be a common feature of breast cancer. These findings, when taken alongside our findings in the mouse model, indicate a role for ATF2-dependent transcription in tumor suppression.

DISCUSSION

ATF2 functions in a context-dependent manner to either promote or antagonize tumorigenesis. In this study, we show that ATF2 inhibits anchorage-independent growth of cells transformed by oncogenic Ras and suppresses tumor formation in a mouse model of liver cancer. This suppression requires phosphorylation of its transactivation domain by JNK. We identify a JNK-ATF2-dependent gene signature that is downregulated in many human tumors, strongly supporting a role for JNK and ATF2 in the inhibition of cancer development in humans. Our observation that JNK suppresses the development of liver tumors is consistent with the results of Das et al. (2011), who demonstrated that hepatocyte-specific deletion of JNK promotes liver tumor formation. Although other groups have shown that JNK can promote liver tumorigenesis (Hui et al., 2008; Sakurai et al., 2006), this effect involves JNK-dependent expression of cytokines in liver stromal cells (Das et al., 2011). Given that ATF2 is an effector of JNK-dependent gene expression, it is possible that ATF2 also influences tumor development by directing transcription in stromal cells. Further studies are needed to address this question. Hyperactivation of Ras signaling, due either to increased expression of HRas or silencing of negative regulatory proteins (Calvisi et al., 2011; Newell et al., 2009), is a common feature of HCC. Its importance in tumor development is underscored by the favorable responses seen in some patients treated with the Raf kinase inhibitor sorafenib (Galmiche et al., 2014). In addition, activating mutations in HRas are frequently detected in mouse liver tumors induced by chemical carcinogens (Jaworski et al., 2005).These observations support the relevance of the Ras-driven HCC model we have used in these studies of ATF2. However, it will be of interest to determine

Figure 3. JNK Suppresses HRasV12-Dependent Transformation and Tumorigenesis via ATF2

(A) Anchorage-independent growth of HRasV12-transformed NIH 3T3 cells expressing GFP, JNK1-CA, or JNK-KD as indicated. ± SD; n = 18; *$p < 0.05$.

(B) Anchorage-independent growth of HRasV12-transformed *Atf2* WT and KO hepatoblasts expressing GFP, JNK1-CA, or JNK-KD as indicated. ± SD; n = 18; *$p < 0.05$.

(C) As in (B), except *Atf2* WT and KO MEFs were used. ± SD; n = 18; *$p < 0.05$.

(D) Anchorage-independent growth of HRasV12-transformed *Atf2* KO hepatoblasts expressing GFP, ATF2, JNK1-CA, and JNK1-KD as indicated. ± SD; n = 18; *$p < 0.05$.

(E) Liver tumor formation in mice injected with HRasV12-transformed *Atf2* KO hepatoblasts expressing GFP, ATF2, and JNK1-CA as indicated; n = 5.

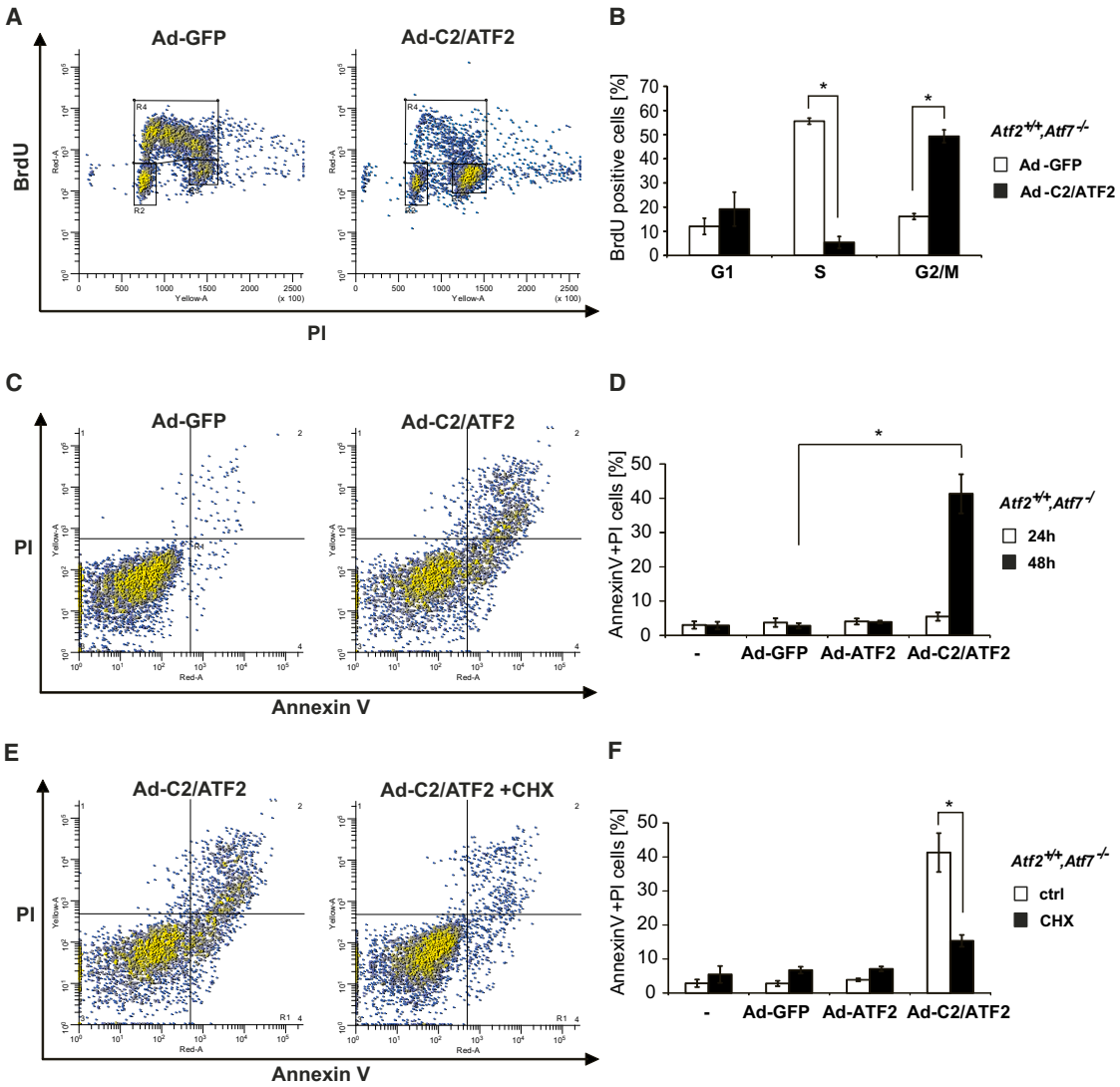

Figure 4. Active ATF2 Blocks Cellular Proliferation and Causes Apoptosis

(A) *Atf2* WT hepatoblasts were transduced with adenoviruses expressing either GFP or C2/ATF2 and harvested for cell-cycle analysis by FACS 16 hr later. Typical results are shown.

(B) Quantification of (A). ± SD; n = 3; *p < 0.05.

(C) *Atf2* WT hepatoblasts expressing either GFP or C2/ATF2 were harvested 48 hr after viral transduction, and apoptosis was assessed by FACS. Typical results are shown.

(D) Quantification of (C). ± SD; n = 3; *p < 0.05.

(E) *Atf2* WT hepatoblasts were transduced with adenoviruses expressing either GFP or C2/ATF2, treated with cycloheximide (CHX) or vehicle control, and harvested for FACS analysis 48 hr later.

(F) Quantification of (E). ± SD; n = 3; *p < 0.05.

whether ATF2 can also suppress tumor formation driven by other oncogenes implicated in HCC such as beta-catenin.

We selected six ATF2-dependent target genes identified by microarray and tested their ability to impair RasV12-dependent transformation. Exogenous expression of three genes, *PPP2R5B*, *GABRA1*, and *RCAN1*, blocked anchorage-independent growth of Ras-transformed MEFs, effectively reversing the enhanced colony formation observed in ATF2 KO cells. PPP2R5B encodes a PP2A-regulatory subunit belonging to the B56 family of proteins (Arnold and Sears, 2008). We show that its overexpression impaired proliferation of MEFs transformed by oncogenic Ras and caused an accumulation of cells in G1. Two substrates have been identified for the B56b-containing PP2A holoenzyme: it regulates Akt phosphorylation in the context of insulin signaling (Rodgers et al., 2011) and interacts with the proto-oncogene, Pim-1, mediating its dephosphorylation and subsequent degradation (Ma et al., 2007). Both Akt and Pim-1 are pro-oncogenic kinases, and it will be of interest

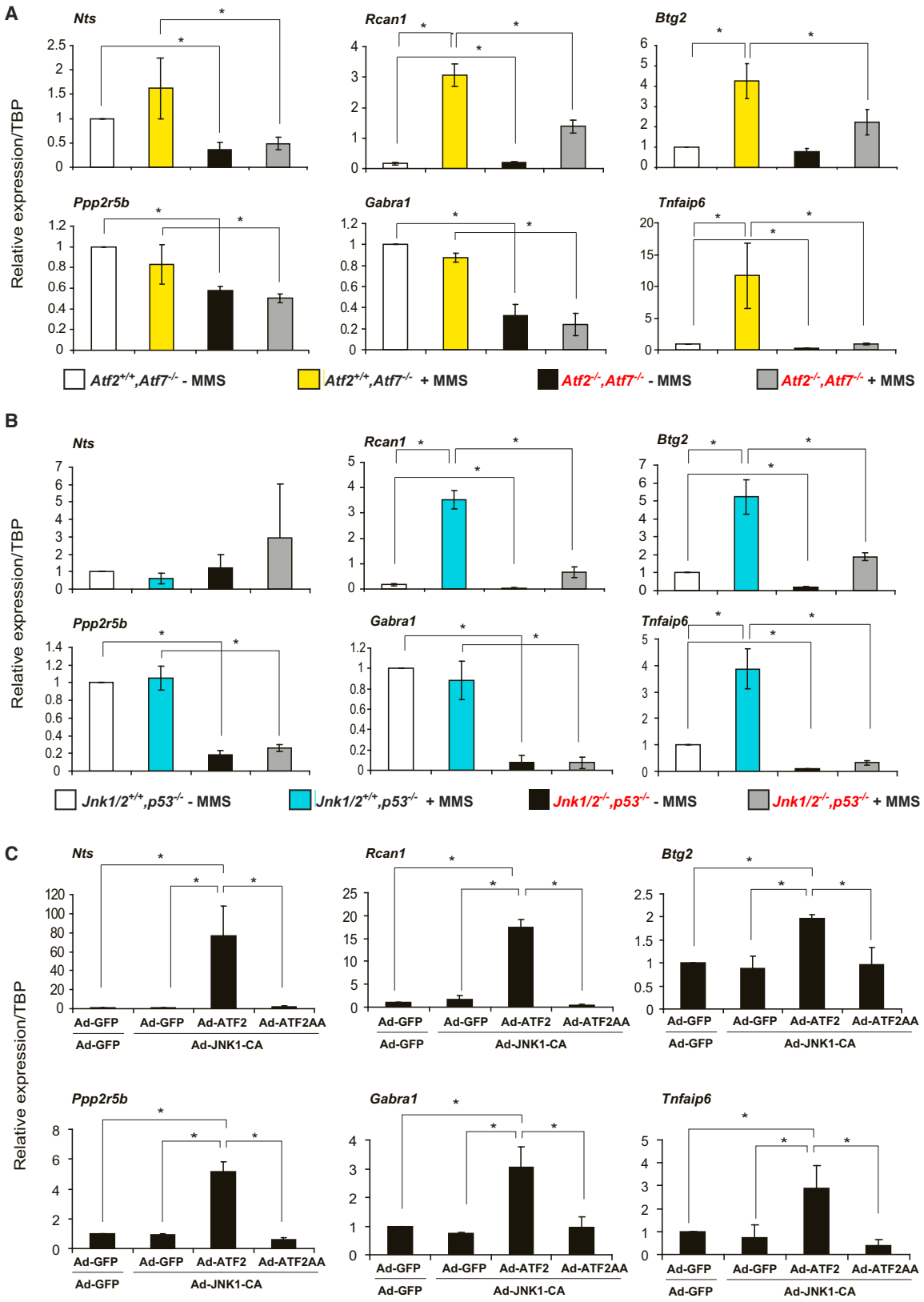

(legend on next page)

to determine whether JNK and ATF2 can regulate their function via B56b expression. *GABRA1* encodes the alpha 1 subunit of the GABA receptor. Methylation of the *GABRA1* promoter region has been detected in a cohort of colorectal tumors, with an accompanying drop in expression (Lee et al., 2012). In addition, loss of GABRA function in brain tumors is frequently seen and loss of expression is particularly striking in glioblastoma (Labrakakis et al., 1998). This would be consistent with a suppressive role for *GABRA1* in the development of such tumors. *RCAN1* (also known as DSCR1—Down syndrome critical region 1) encodes a regulator of the calcium-dependent phosphatase calcineurin, which in turn activates the NFAT family of transcription factors. *RCAN1* is a candidate tumor suppressor that can impede angiogenesis by inhibiting the proliferation of endothelial cells (Baek et al., 2009). We found that exogenous expression of RCAN1 inhibited proliferation of Ras-transformed MEFs, which may explain its ability to inhibit anchorage-independent growth of these cells. Analysis of Oncomine data sets revealed that RCAN1 is significantly underexpressed in HCCs and a range of other tumor types, implying that increased calcineurin-NFAT signaling may occur in many tumors. Indeed, aberrant NFAT function has been implicated in the proliferation and survival of several tumor types including liver cancer (Müller and Rao, 2010; Wang et al., 2012). Interestingly, the calcineurin-NFAT- and JNK-signaling pathways are known to be coordinately regulated: calcineurin interacts with, and activates, ASK-1, leading to activation of JNK. On the other hand, phosphorylation of NFAT proteins by JNK inhibits their translocation to the nucleus (Chow et al., 1997). Therefore, the activation of *RCAN1* transcription by ATF2 may represent another layer of control exercised by JNK over NFAT function. To date, we have characterized the response of Ras-transformed cells to just six of the genes identified in the microarray data, and we anticipate that several other ATF2-dependent genes contribute to the antioncogenic effects described in this study. Indeed, we cannot rule out the possibility that ATF2 promotes expression of other JNK substrates that participate in tumor suppression. Furthermore, it should be noted that JNK may regulate ATF2 function by phosphorylating other factors present in the ATF2-transcription complex.

The analysis of various gene-expression tumor data sets highlights a strong tendency for ATF2 targets to be underexpressed in hepatocellular carcinoma and several other tumor types. Intriguingly, there is widespread underexpression of JNK-ATF2 transcriptional targets in breast tumors. Notably, loss of ATF2 function is sufficient to promote breast tumor formation: Maekawa et al. (2007, 2008) report the spontaneous development of mammary tumors in ATF2 heterozygous mice, which they attribute to impaired expression of maspin and GADD45a in ATF2 heterozygous (and knockout) MEFs and tumors. Furthermore, histological analysis of human breast tumors by Knippen et al. (2009) demonstrated that high expression of phosphorylated (and therefore transcriptionally active) ATF2 correlated with prolonged survival. These findings are consistent with a tumor-suppressive role for ATF2 in breast. Our findings raise the possibility that several ATF2-dependent target genes may be involved in actively suppressing breast tumor formation.

At this stage, we do not know how downregulation of ATF2-dependent gene expression in tumors occurs. One possibility is that somatic mutations in JNK, or its upstream kinases, leads to impaired ATF2 activation. As yet, however, the impact of cancer-associated mutations in stress-signaling kinases on ATF2 function remains to be examined. Another possibility is that epigenetic silencing of ATF2 targets occurs during tumor development. The SS18-SSX fusion protein provides a specific example of oncogenesis, involving epigenetic regulation of ATF2 targets. In synovial sarcomas, SS18-SSX forms a protein complex with TLE1 and DNA-associated ATF2. This targets the epigenetic corepressor function of TLE1 to ATF2 target promoters and silences transcription—an effect that is required for the oncogenic function of the fusion protein (Su et al., 2012). In principle, therefore, epigenetic inhibition of ATF2 transcription could promote tumor development in other settings, and there is widespread evidence that enzymes involved in epigenetic modification of chromatin often function aberrantly in tumor cells, leading to alterations in transcriptional programs.

In summary, our data indicate that JNK and ATF2 cooperate to drive a transcriptional program that can suppress tumor development. Further studies are ongoing to define in detail the nature of this program.

EXPERIMENTAL PROCEDURES

Reagents

The following cell lines were employed: NIH 3T3 (American Type Culture Collection; LGC Standards UK); *Jnk1/2*$^{+/+}$, *p53*$^{-/-}$ and *Jnk1/2*$^{-/-}$,*p53*$^{-/-}$ MEFs (a kind gift of Prof. R.J. Davis); and *p38*$^{+/+}$, *p38*$^{-/-}$ MEFs (a kind gift of Prof. A. Nebreda). Cultivation of hepatoblasts and MEFs is described in the Supplemental Experimental Procedures. MKK6EE (Raingeaud et al., 1996) and MKK7-JNK1 (Lei et al., 2002) coding sequences were obtained from Addgene.

Cre-Mediated Deletion of ATF2 Sequences

Ad-GFP and Ad-CRE-GFP virus stocks were obtained from Gene Transfer Vector Core (University of Iowa). Cells were incubated with 0.5–1 μl of virus in serum-free Dulbecco's modified Eagle's medium (DMEM) for 30–60 min at 37°C. Cells were sorted for GFP expression 24–48 hr post-infection by fluorescence-activated cell sorting (FACS) and expanded in culture.

Mice, Chimeric Mouse Model for Hepatocellular Carcinoma

In vivo experiments were approved by the Cancer Research UK (CRUK) Manchester Institute Animal Ethics Committee and performed under a project license issued by the United Kingdom Home Office, in keeping with the Animal Scientific Procedures Act 1986. C57BL/6 mice were purchased from Harlan. *ATF2*$^{f/f}$ and *ATF7*$^{-/-}$ mice are described in a previous report (Breitwieser et al., 2007). The chimeric mouse model for hepatocellular carcinoma is described in (Zender et al., 2006) and in Supplemental Experimental

Figure 5. Identification of Genes Expressed in an ATF2- and JNK-Dependent Manner

(A) Gene expression was assessed by qPCR of RNA from *Atf2* WT and KO hepatoblasts treated with 1 mM MMS or vehicle control for 3 hr; ± SD; n = 3; *p < 0.05.

(B) As in (A), except JNK1/2 WT and JNK1/2 KO MEFs were compared; ± SD; n = 3; *p < 0.05.

(C) Gene expression was assessed by qPCR of RNA from *Atf2* KO hepatoblasts transduced with adenoviruses expressing GFP, ATF2, ATF2AA, and JNK1-CA in the indicated combinations; ± SD; n = 3; *p < 0.05.

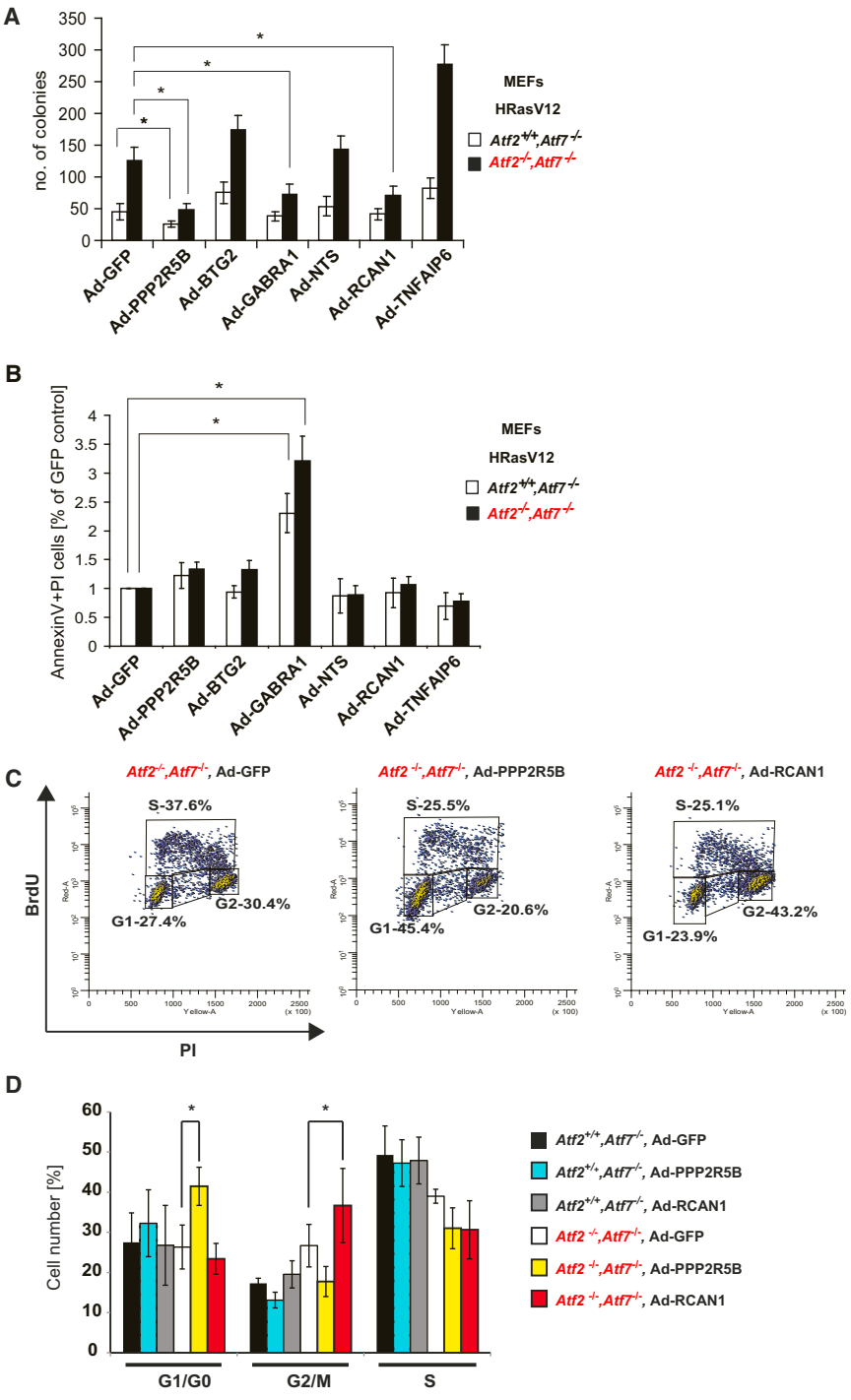

Figure 6. Inhibition of Cellular Transformation by Selected JNK-ATF2-Dependent Targets Genes

(A) Anchorage-independent growth of HRasV12-transformed *Atf2* WT and KO MEFs expressing the indicated ATF2-dependent target genes. ± SD; n = 18; *p < 0.05.

(B) *Atf2* WT and KO MEFs were transduced with adenoviruses expressing the indicated ATF2-dependent target genes, and apoptosis was assessed by FACS 48 hr later. ± SD; n = 3; *p < 0.05.

(C) *Atf2* WT and KO MEFs were transduced with adenoviruses expressing the indicated ATF2-dependent target genes and harvested for cell cycle analysis by FACS. The FACS plots show typical results obtained when either PPP2R5B or RCAN1 is expressed in *Atf2* KO MEFs.

(D) Quantification of (C). ± SD; n = 3; *p < 0.05.

Procedures. Imaging of tumors in vivo is described in Supplemental Experimental Procedures.

Cell Growth and Colony Formation in Soft Agar

To assess their adherent growth rate, cells were plated at 8,000/well on 24-well plates and cultured for 5 days. Cell density was measured daily by staining with 0.1% crystal violet. Crystal violet was subsequently dissolved in 2% SDS, and absorbance at λ = 595 nm was measured. To assess growth in soft agar, cells were seeded in a semisolid medium comprising 0.35% agarose in DMEM and 10% fetal bovine serum (FBS) (5,000/well of a 6-well plate). One milliliter of this suspension was overlaid onto a base layer of 0.5% agarose in DMEM 10% FBS. The plates were incubated for 14 days and stained with iodonitrotetrazolium chloride (0.5 mg/ml) overnight. Colonies were counted by processing scanned images using ImageJ software.

ROS Measurement

To assess intracellular ROS levels, $p38^{+/+}$ and $p38^{-/-}$ MEFs were stained with dihydroethidium (DHE) (10 μg/ml) for 30 min and trypsinized, and the mean fluorescence was measured by FACS.

Kinase Inhibitors

JNK inhibitors SP600125 (Tocris Bioscience; 1496), BI-87G3 (Calbiochem; 420142), and MEK inhibitor PD98058 (Tocris Bioscience; 1213) were used at a final concentration of 10 μM. DMSO (Sigma; D2650) was used as a vehicle control for each inhibitor.

Cell Cycle and Apoptosis Assays

Cells were labeled with bromodeoxyuridine (BrdU) for 15 min and fixed in 70% ethanol. Histones were extracted in 0.1M HCl and 0.5% Triton X-100 for 10 min on ice. After resuspension in water, cells were heated to 95°C for 10 min and then cooled on ice. PBS/0.5% Triton was used for permeabilization. To stain, cells were incubated with anti-BrdU (Roche; 11170376001) diluted in PBS/0.1% BSA. Detection was via a fluorescent goat anti-mouse secondary antibody (Life Technologies; A21236). Apoptosis was measured by FACS analysis of Annexin V (Biolegend; 640912) and phosphatidylinositol-stained cells (25 μg/ml; Sigma; P4864). For cycloheximide treatment, Ad-C2/ATF2-infected cells were treated with 3 μM of cyclohexamide (Sigma; C4859) and apoptosis was measured 48 hr later.

qPCR and ChIP

RNA was extracted using a GenElute Total RNA extraction kit (Sigma; RTN350). cDNA synthesis was performed using a Quantitect reverse transcription kit (QIAGEN; 205313). Quantitative PCR was performed using Jumpstart qPCR ready mix for probes (Sigma D6442) and the Universal Probe Library

A

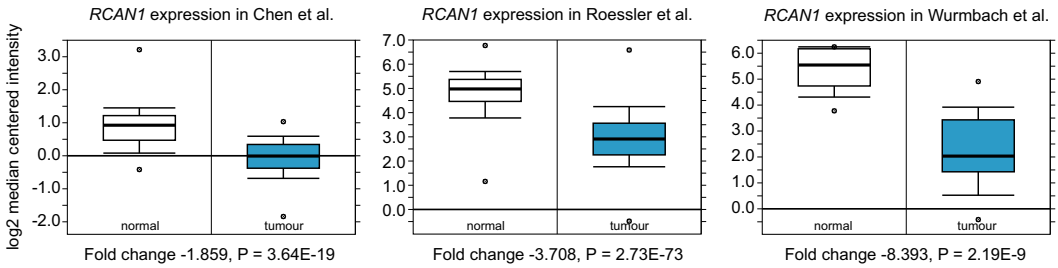

B

Rank	P-value	Fold Change	Gene
29	2.83E-40	-2.53	CREB5
178	6.20E-30	-2.58	SLC25A25
361	6.69E-25	-5.07	PAMR1
533	4.45E-22	-5.02	RCAN1
943	1.23E-17	-5.66	ATF3
976	2.32E-17	-7.79	KRT17
1110	3.55E-16	-1.60	DENND5B
1258	4.67E-15	-4.39	EGR2
1326	1.40E-14	-2.87	PDLIM3
1337	1.62E-14	-1.76	NR4A3
1479	2.12E-13	-1.36	MCAM
1528	4.43E-13	-1.70	DAAM1
1545	5.77E-13	-1.28	PPP2R5B
2200	1.18E-9	-1.33	ANGPTL1
3009	7.26E-7	-1.21	ATP6V0A4
3367	5.47E-6	-1.09	CALCA
4020	9.81E-5	-1.46	BTG2
4650	7.12E-4	-1.47	TNFAIP6
6927	0.045	-1.12	DGAT1
7490	0.085	-1.02	NTS

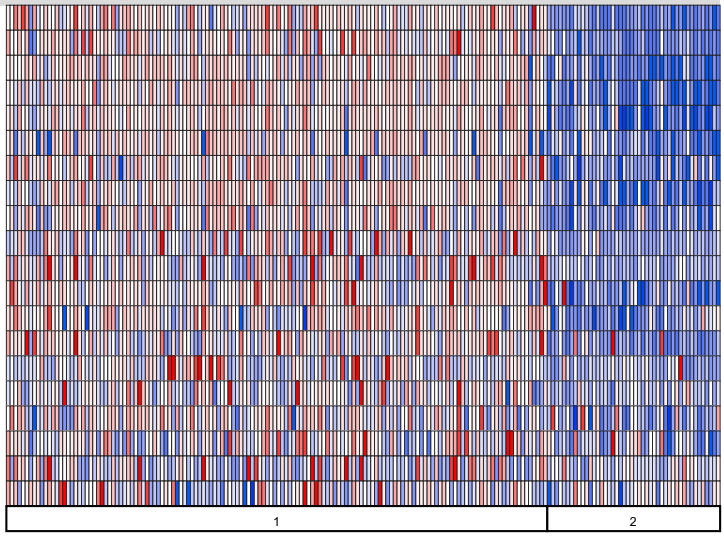

1 - breast tissue (n=144)
2 - mucinous breast carcinoma (n=46)

C

p-Value	Gene
1.40E-63	CREB5
6.20E-30	SLC25A25
1.76E-7	PAMR1
4.54E-35	ATF3
4.45E-22	RCAN1
1.17E-29	EGR2
4.19E-24	DENND5B
1.95E-38	ANGPTL1
2.12E-13	MCAM
4.02E-4	NR4A3
1.96E-15	DAAM1
9.13E-15	KRT17
1.61E-15	PDLIM3
4.01E-23	PPP2R5B
0.006	BTG2
2.03E-4	CALCA
1.98E-4	ATP6V0A4
2.46E-4	DGAT1
0.036	ATP6V0A1
0.208	STMN4

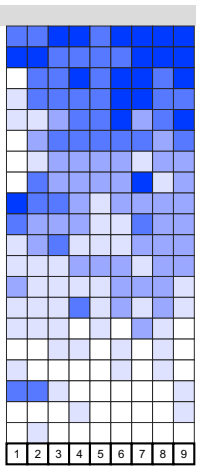

1 - Breast Phyllodes tumour vs normal
2 - Ductal Breast Carcinoma In Situ vs normal
3 - Invasive Breast Carcinoma vs normal
4 - Invasive Ductal Breast Carcinoma vs normal
5 - Invasive Ductal and Invasive Lobular Breast Carcinoma vs normal
6 - Invasive Lobular Breast Carcinoma vs normal
7 - Medullary Breast Carcinoma vs normal
8 - Mucinous Breast Carcinoma vs normal
9 - Tubular Breast Carcinoma vs normal

D

p-Value	Gene
7.65E-19	CREB5
6.44E-12	PAMR1
1.86E-34	RCAN1
5.35E-12	SLC25A25
2.54E-8	ATF3
2.04E-12	ANGPTL1
2.54E-8	EGR2
2.77E-21	DENND5B
0.001	MCAM
1.32E-12	PDLIM3
6.20E-16	NR4A3
6.71E-9	KRT17
1.74E-5	DAAM1
4.93E-5	BTG2
0.019	CALCA
0.022	PPP2R5B
0.091	CFTR
0.025	ATP6V0A4
9.12E-4	STMN4
0.043	NTS

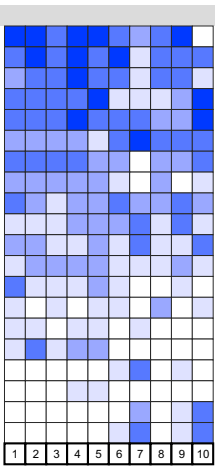

1 - Curtis et al. Invasive breast carcinoma vs normal
2 - Curtis et al. Invasive ductal and invasive lobular carcinoma vs normal
3 - Curtis et al. Invasive ductal carcinoma vs normal
4 - Curtis et al. Invasive lobular carcinoma vs normal
5 - Curtis et al. Mucinous breast carcinoma vs normal
6 - TGCA Invasive breast carcinoma vs normal
7 - TGCA Invasive ductal and invasive lobular carcinoma vs normal
8 - TGCA Invasive ductal carcinoma vs normal
9 - TGCA Invasive lobular carcinoma vs normal
10 - TGCA Mucinous breast carcinoma vs normal

least expressed **most expressed**

(legend on next page)

system (Roche). TBP and TAF6 housekeeper genes were used for normalization of data. ChIP was performed using an ATF2-specific antibody (E243; Millipore; 04-1021) and Simple ChIP reagents (Cell Signaling Technology no. 9002), according to manufacturer's instructions. qPCR and ChIP primer sequences are presented in Table S6.

Oncomine

Oncomine was used for analysis and visualization of JNK- and ATF2-dependent transcripts in normal and tumor samples (https://www.oncomine.org/resource/login.html; Thermo Fisher Scientific).

ACCESSION NUMBERS

The data have been uploaded to the Gene Expression Omnibus, accession no. GSE50530. Details are in the Supplemental Experimental Procedures.

SUPPLEMENTAL INFORMATION

Supplemental Information includes Supplemental Experimental Procedures, four figures, and six tables and can be found with this article online at http://dx.doi.org/10.1016/j.celrep.2014.10.043.

AUTHOR CONTRIBUTIONS

M.G. and S.L. designed and carried out experiments and prepared the manuscript. S.K. carried out experiments and assisted in manuscript preparation. J.T. and Y.L. carried out analysis of microarray and ChIP-seq data. J.W. assisted in experimental work. G.T. designed and characterized C2/ATF2. W.B. designed ATF2 knockout strategy and mouse breeding. N.J. designed the study, supervised the team, and prepared the manuscript.

ACKNOWLEDGMENTS

We would like to thank Professor Roger Davis, Professor Angel Nebreda, Professor Scott Lowe, and Dr. David Gilham for kindly providing reagents. We thank the staff of the CRUK Manchester Institute Biological Resource Unit, Molecular Biology Core Facility, and FACS department for their excellent support. We are grateful to Dr. John Brognard for his critical reading of the manuscript. This work was funded by Cancer Research UK.

Received: September 3, 2013
Revised: July 16, 2014
Accepted: October 14, 2014
Published: November 13, 2014

REFERENCES

Arnold, H.K., and Sears, R.C. (2008). A tumor suppressor role for PP2A-B56alpha through negative regulation of c-Myc and other key oncoproteins. Cancer Metastasis Rev. *27*, 147–158.

Baek, K.H., Zaslavsky, A., Lynch, R.C., Britt, C., Okada, Y., Siarey, R.J., Lensch, M.W., Park, I.H., Yoon, S.S., Minami, T., et al. (2009). Down's syndrome suppression of tumour growth and the role of the calcineurin inhibitor DSCR1. Nature *459*, 1126–1130.

Berger, A.J., Kluger, H.M., Li, N., Kielhorn, E., Halaban, R., Ronai, Z., and Rimm, D.L. (2003). Subcellular localization of activating transcription factor 2 in melanoma specimens predicts patient survival. Cancer Res. *63*, 8103–8107.

Bhoumik, A., Fichtman, B., Derossi, C., Breitwieser, W., Kluger, H.M., Davis, S., Subtil, A., Meltzer, P., Krajewski, S., Jones, N., and Ronai, Z. (2008). Suppressor role of activating transcription factor 2 (ATF2) in skin cancer. Proc. Natl. Acad. Sci. USA *105*, 1674–1679.

Breitwieser, W., Lyons, S., Flenniken, A.M., Ashton, G., Bruder, G., Willington, M., Lacaud, G., Kouskoff, V., and Jones, N. (2007). Feedback regulation of p38 activity via ATF2 is essential for survival of embryonic liver cells. Genes Dev. *21*, 2069–2082.

Calvisi, D.F., Ladu, S., Conner, E.A., Seo, D., Hsieh, J.T., Factor, V.M., and Thorgeirsson, S.S. (2011). Inactivation of Ras GTPase-activating proteins promotes unrestrained activity of wild-type Ras in human liver cancer. J. Hepatol. *54*, 311–319.

Cellurale, C., Weston, C.R., Reilly, J., Garlick, D.S., Jerry, D.J., Sluss, H.K., and Davis, R.J. (2010). Role of JNK in a Trp53-dependent mouse model of breast cancer. PLoS ONE *5*, e12469.

Cellurale, C., Sabio, G., Kennedy, N.J., Das, M., Barlow, M., Sandy, P., Jacks, T., and Davis, R.J. (2011). Requirement of c-Jun NH(2)-terminal kinase for Ras-initiated tumor formation. Mol. Cell. Biol. *31*, 1565–1576.

Cellurale, C., Girnius, N., Jiang, F., Cavanagh-Kyros, J., Lu, S., Garlick, D.S., Mercurio, A.M., and Davis, R.J. (2012). Role of JNK in mammary gland development and breast cancer. Cancer Res. *72*, 472–481.

Chen, X., Cheung, S.T., So, S., Fan, S.T., Barry, C., Higgins, J., Lai, K.M., Ji, J., Dudoit, S., Ng, I.O., et al. (2002). Gene expression patterns in human liver cancers. Mol. Biol. Cell *13*, 1929–1939.

Chow, C.W., Rincón, M., Cavanagh, J., Dickens, M., and Davis, R.J. (1997). Nuclear accumulation of NFAT4 opposed by the JNK signal transduction pathway. Science *278*, 1638–1641.

Curtis, C., Shah, S.P., Chin, S.F., Turashvili, G., Rueda, O.M., Dunning, M.J., Speed, D., Lynch, A.G., Samarajiwa, S., Yuan, Y., et al.; METABRIC Group (2012). The genomic and transcriptomic architecture of 2,000 breast tumours reveals novel subgroups. Nature *486*, 346–352.

Das, M., Garlick, D.S., Greiner, D.L., and Davis, R.J. (2011). The role of JNK in the development of hepatocellular carcinoma. Genes Dev. *25*, 634–645.

Dolado, I., Swat, A., Ajenjo, N., De Vita, G., Cuadrado, A., and Nebreda, A.R. (2007). p38alpha MAP kinase as a sensor of reactive oxygen species in tumorigenesis. Cancer Cell *11*, 191–205.

Eferl, R., Ricci, R., Kenner, L., Zenz, R., David, J.P., Rath, M., and Wagner, E.F. (2003). Liver tumor development. c-Jun antagonizes the proapoptotic activity of p53. Cell *112*, 181–192.

Esteva, F.J., Sahin, A.A., Smith, T.L., Yang, Y., Pusztai, L., Nahta, R., Buchholz, T.A., Buzdar, A.U., Hortobagyi, G.N., and Bacus, S.S. (2004). Prognostic significance of phosphorylated P38 mitogen-activated protein kinase and HER-2 expression in lymph node-positive breast carcinoma. Cancer *100*, 499–506.

Galmiche, A., Chauffert, B., and Barbare, J.C. (2014). New biological perspectives for the improvement of the efficacy of sorafenib in hepatocellular carcinoma. Cancer Lett. *346*, 159–162.

Greenman, C., Stephens, P., Smith, R., Dalgliesh, G.L., Hunter, C., Bignell, G., Davies, H., Teague, J., Butler, A., Stevens, C., et al. (2007). Patterns of somatic mutation in human cancer genomes. Nature *446*, 153–158.

Figure 7. Underexpression of ATF2-Dependent Transcripts in Human Tumors

(A) RCAN1 mRNA expression in normal liver compared to hepatocellular carcinoma. Graphs were produced from published data (Chen et al., 2002; Roessler et al., 2010; Wurmbach et al., 2007).

(B) Expression of an ATF2-dependent gene signature in normal breast compared to mucinous breast carcinoma using published data (Curtis et al., 2012).

(C) Underexpression of ATF2-dependent transcripts in several breast tumor types versus normal breast. Heatmap produced using published data (Curtis et al., 2012).

(D) Underexpression of ATF2-dependent transcripts in breast tumors versus normal breast using data from two independent sources: Curtis et al. (2012) and TGCA (https://tcga-data.nci.nih.gov/tcga/).

(A–D) Analysis performed using the Oncomine database.

Gupta, S., Campbell, D., Dérijard, B., and Davis, R.J. (1995). Transcription factor ATF2 regulation by the JNK signal transduction pathway. Science *267*, 389–393.

Hübner, A., Mulholland, D.J., Standen, C.L., Karasarides, M., Cavanagh-Kyros, J., Barrett, T., Chi, H., Greiner, D.L., Tournier, C., Sawyers, C.L., et al. (2012). JNK and PTEN cooperatively control the development of invasive adenocarcinoma of the prostate. Proc. Natl. Acad. Sci. USA *109*, 12046–12051.

Hui, L., Bakiri, L., Mairhorfer, A., Schweifer, N., Haslinger, C., Kenner, L., Komnenovic, V., Scheuch, H., Beug, H., and Wagner, E.F. (2007). p38alpha suppresses normal and cancer cell proliferation by antagonizing the JNK-c-Jun pathway. Nat. Genet. *39*, 741–749.

Hui, L., Zatloukal, K., Scheuch, H., Stepniak, E., and Wagner, E.F. (2008). Proliferation of human HCC cells and chemically induced mouse liver cancers requires JNK1-dependent p21 downregulation. J. Clin. Invest. *118*, 3943–3953.

Jaworski, M., Buchmann, A., Bauer, P., Riess, O., and Schwarz, M. (2005). B-raf and Ha-ras mutations in chemically induced mouse liver tumors. Oncogene *24*, 1290–1295.

Knippen, S., Löning, T., Müller, V., Schröder, C., Jänicke, F., and Milde-Langosch, K. (2009). Expression and prognostic value of activating transcription factor 2 (ATF2) and its phosphorylated form in mammary carcinomas. Anticancer Res. *29*, 183–189.

Labrakakis, C., Patt, S., Hartmann, J., and Kettenmann, H. (1998). Functional GABA(A) receptors on human glioma cells. Eur. J. Neurosci. *10*, 231–238.

Lee, S., Oh, T., Chung, H., Rha, S., Kim, C., Moon, Y., Hoehn, B.D., Jeong, D., Lee, S., Kim, N., et al. (2012). Identification of GABRA1 and LAMA2 as new DNA methylation markers in colorectal cancer. Int. J. Oncol. *40*, 889–898.

Lei, K., Nimnual, A., Zong, W.X., Kennedy, N.J., Flavell, R.A., Thompson, C.B., Bar-Sagi, D., and Davis, R.J. (2002). The Bax subfamily of Bcl2-related proteins is essential for apoptotic signal transduction by c-Jun NH(2)-terminal kinase. Mol. Cell. Biol. *22*, 4929–4942.

Ma, J., Arnold, H.K., Lilly, M.B., Sears, R.C., and Kraft, A.S. (2007). Negative regulation of Pim-1 protein kinase levels by the B56beta subunit of PP2A. Oncogene *26*, 5145–5153.

Maekawa, T., Shinagawa, T., Sano, Y., Sakuma, T., Nomura, S., Nagasaki, K., Miki, Y., Saito-Ohara, F., Inazawa, J., Kohno, T., et al. (2007). Reduced levels of ATF-2 predispose mice to mammary tumors. Mol. Cell. Biol. *27*, 1730–1744.

Maekawa, T., Sano, Y., Shinagawa, T., Rahman, Z., Sakuma, T., Nomura, S., Licht, J.D., and Ishii, S. (2008). ATF-2 controls transcription of Maspin and GADD45 alpha genes independently from p53 to suppress mammary tumors. Oncogene *27*, 1045–1054.

Müller, M.R., and Rao, A. (2010). NFAT, immunity and cancer: a transcription factor comes of age. Nat. Rev. Immunol. *10*, 645–656.

Newell, P., Toffanin, S., Villanueva, A., Chiang, D.Y., Minguez, B., Cabellos, L., Savic, R., Hoshida, Y., Lim, K.H., Melgar-Lesmes, P., et al. (2009). Ras pathway activation in hepatocellular carcinoma and anti-tumoral effect of combined sorafenib and rapamycin in vivo. J. Hepatol. *51*, 725–733.

Raingeaud, J., Whitmarsh, A.J., Barrett, T., Dérijard, B., and Davis, R.J. (1996). MKK3- and MKK6-regulated gene expression is mediated by the p38 mitogen-activated protein kinase signal transduction pathway. Mol. Cell. Biol. *16*, 1247–1255.

Rodgers, J.T., Vogel, R.O., and Puigserver, P. (2011). Clk2 and B56β mediate insulin-regulated assembly of the PP2A phosphatase holoenzyme complex on Akt. Mol. Cell *41*, 471–479.

Roessler, S., Jia, H.L., Budhu, A., Forgues, M., Ye, Q.H., Lee, J.S., Thorgeirsson, S.S., Sun, Z., Tang, Z.Y., Qin, L.X., and Wang, X.W. (2010). A unique metastasis gene signature enables prediction of tumor relapse in early-stage hepatocellular carcinoma patients. Cancer Res. *70*, 10202–10212.

Sakurai, T., Maeda, S., Chang, L., and Karin, M. (2006). Loss of hepatic NF-kappa B activity enhances chemical hepatocarcinogenesis through sustained c-Jun N-terminal kinase 1 activation. Proc. Natl. Acad. Sci. USA *103*, 10544–10551.

Salh, B., Marotta, A., Wagey, R., Sayed, M., and Pelech, S. (2002). Dysregulation of phosphatidylinositol 3-kinase and downstream effectors in human breast cancer. Int. J. Cancer *98*, 148–154.

Shah, M., Bhoumik, A., Goel, V., Dewing, A., Breitwieser, W., Kluger, H., Krajewski, S., Krajewska, M., Dehart, J., Lau, E., et al. (2010). A role for ATF2 in regulating MITF and melanoma development. PLoS Genet. *6*, e1001258.

Shibata, W., Maeda, S., Hikiba, Y., Yanai, A., Sakamoto, K., Nakagawa, H., Ogura, K., Karin, M., and Omata, M. (2008). c-Jun NH2-terminal kinase 1 is a critical regulator for the development of gastric cancer in mice. Cancer Res. *68*, 5031–5039.

Stark, M.S., Woods, S.L., Gartside, M.G., Bonazzi, V.F., Dutton-Regester, K., Aoude, L.G., Chow, D., Sereduk, C., Niemi, N.M., Tang, N., et al. (2012). Frequent somatic mutations in MAP3K5 and MAP3K9 in metastatic melanoma identified by exome sequencing. Nat. Genet. *44*, 165–169.

Steinmüller, L., and Thiel, G. (2003). Regulation of gene transcription by a constitutively active mutant of activating transcription factor 2 (ATF2). Biol. Chem. *384*, 667–672.

Stephens, P.J., Tarpey, P.S., Davies, H., Van Loo, P., Greenman, C., Wedge, D.C., Nik-Zainal, S., Martin, S., Varela, I., Bignell, G.R., et al.; Oslo Breast Cancer Consortium (OSBREAC) (2012). The landscape of cancer genes and mutational processes in breast cancer. Nature *486*, 400–404.

Su, L., Sampaio, A.V., Jones, K.B., Pacheco, M., Goytain, A., Lin, S., Poulin, N., Yi, L., Rossi, F.M., Kast, J., et al. (2012). Deconstruction of the SS18-SSX fusion oncoprotein complex: insights into disease etiology and therapeutics. Cancer Cell *21*, 333–347.

Thomas, D.J., Rosenbloom, K.R., Clawson, H., Hinrichs, A.S., Trumbower, H., Raney, B.J., Karolchik, D., Barber, G.P., Harte, R.A., Hillman-Jackson, J., et al.; ENCODE Project Consortium (2007). The ENCODE Project at UC Santa Cruz. Nucleic Acids Res. *35*, D663–D667.

Ventura, J.J., Tenbaum, S., Perdiguero, E., Huth, M., Guerra, C., Barbacid, M., Pasparakis, M., and Nebreda, A.R. (2007). p38alpha MAP kinase is essential in lung stem and progenitor cell proliferation and differentiation. Nat. Genet. *39*, 750–758.

Wagner, E.F., and Nebreda, A.R. (2009). Signal integration by JNK and p38 MAPK pathways in cancer development. Nat. Rev. Cancer *9*, 537–549.

Walczynski, J., Lyons, S., Jones, N., and Breitwieser, W. (2014). Sensitisation of c-MYC-induced B-lymphoma cells to apoptosis by ATF2. Oncogene *33*, 1027–1036.

Wang, S., Kang, X., Cao, S., Cheng, H., Wang, D., and Geng, J. (2012). Calcineurin/NFATc1 pathway contributes to cell proliferation in hepatocellular carcinoma. Dig. Dis. Sci. *57*, 3184–3188.

Wurmbach, E., Chen, Y.B., Khitrov, G., Zhang, W., Roayaie, S., Schwartz, M., Fiel, I., Thung, S., Mazzaferro, V., Bruix, J., et al. (2007). Genome-wide molecular profiles of HCV-induced dysplasia and hepatocellular carcinoma. Hepatology *45*, 938–947.

Yang, Y.M., Bost, F., Charbono, W., Dean, N., McKay, R., Rhim, J.S., Depatie, C., and Mercola, D. (2003). C-Jun NH(2)-terminal kinase mediates proliferation and tumor growth of human prostate carcinoma. Clin. Cancer Res. *9*, 391–401.

Zender, L., Spector, M.S., Xue, W., Flemming, P., Cordon-Cardo, C., Silke, J., Fan, S.T., Luk, J.M., Wigler, M., Hannon, G.J., et al. (2006). Identification and validation of oncogenes in liver cancer using an integrative oncogenomic approach. Cell *125*, 1253–1267.